Article

Fluorescent biosensor for phosphate determination based on immobilized polyfluorene-liposomal nanoparticles coupled with Alkaline Phosphatase

Zehra Kahveci, Maria José Martínez-Tomé, Ricardo Mallavia, and C. Reyes Mateo

ACS Appl. Mater. Interfaces, **Just Accepted Manuscript** • DOI: 10.1021/acsami.6b12434 • Publication Date (Web): 14 Dec 2016

Fluorescent Biosensor for Phosphate Determination Based on Immobilized Polyfluorene-Liposomal Nanoparticles Coupled with Alkaline Phosphatase

*Zehra Kahveci, Maria José Martínez-Tomé, Ricardo Mallavia, C.Reyes Mateo**

Instituto de Biología Molecular y Celular, Universidad Miguel Hernández, 03202, Elche, Alicante, Spain

KEYWORDS: alkaline phosphatase inhibitors; biosensor; fluorescent nanoparticles; conjugated polyelectrolytes; lipid vesicles; phosphate ion; p-nitrophenol

ABSTRACT

This work describes the development of a novel fluorescent biosensor based on the inhibition of alkaline phosphatase (ALP). The biosensor is composed of the enzyme ALP and the conjugated cationic polyfluorene HTMA-PFP. The working principle of the biosensor is based on the fluorescence quenching of this polyelectrolyte by p-nitrophenol (PNP), a product of the hydrolisis reaction of p-nitrophenyl phosphate (PNPP) catalyzed by ALP. Since HTMA-PFP forms unstable aggregates in buffer, with low fluorescence efficiency, previous stabilization of the polyelectrolyte was required before the development of the biosensor. HTMA-PFP was stabilized through its interaction with lipid vesicles to obtain stable blue-emitting nanoparticles (NPs). Fluorescent NPs were characterized and the ability to be quenched by PNP was evaluated. These nanoparticles were coupled to ALP and entrapped in a sol–gel matrix to produce a biosensor that can serve as a screening platform to identify ALP inhibitors. The components of the biosensor were examined before and after sol-gel entrapment, and the biosensor was optimized to allow the determination of phosphate ion in aqueous medium.

INTRODUCTION

The enzyme alkaline phosphatase (ALP) nonspecifically catalyzes the hydrolysis of phosphoryl esters in alkaline media. This low biocatalytic selectivity enables the use of the enzyme for a wide range of substrates in enzyme activity assays, one of which is p-nitrophenyl phosphate (PNPP). In the last years, the catalytic activity of ALP has been exploited in the design of immunosensors and biosensors, either for direct monitoring of analytes (enzymes or substrates) or for indirect monitoring of organic (i.e. pesticides) or inorganic salts (i.e. phosphate, heavy metals) which act as inhibitors[1-5]. Studies of ALP activity and screening of its inhibitors are required in clinical diagnosis to develop potential drug therapies for different diseases, as well as in environmental monitoring of pollutants[6]. The choice of the substrates for these analytical applications depends on the transduction methods, i.e. fluorescence, chemiluminescence or amperometry, and on the purpose of the analytical measurements[3]. Various fluorimetric assays and fluorescent biosensors based on ALP activity have been reported using organic dyes, inorganic semiconductor quantum dots (QDs) and carbon quantum dots as fluorimetric indicators[7-9]. Many of these fluorophores suffer drawbacks such as poor stability of dyes or high toxicity of QDs which constitute important concerns for the practical application. Recently, much interest has been generated in synthesizing novel highly-fluorescent conjugated polyelectrolytes (CPEs)[10-12]. CPEs are polymers containing hydrophobic backbone chain of alternating double- and single-bonds, functionalized with ionic side chains[13, 14]. Thanks to this conjugation, π-electrons are delocalized along the backbone, providing collective optical responses as well as amplified signals when comparing to common fluorophores[14, 15]. CPEs and CPE-based nanoparticles have emerged in recent years as fluorescent probes, due to their low cytotoxicity, excellent photostability and good biocompatibility, thereby allowing their use in biomedical

applications such as cell imaging, diagnosis and therapy without risking the cellular viability[16-22]. In addition, they have received great attention as novel materials for the development of sensor and biosensor devices to detect specific molecules, metal ions and biomolecules [23-26].

The amplified quenching of CPEs upon binding to an opposite charge molecule is frequently used in the design of CPEs-based sensors or biosensors[13, 18, 24, 27]. Chen et al. demonstrated that the fluorescence of the CPEs, can be very efficiently quenched via a photo-induced electron transfer mechanism (PET), by electron acceptors of opposite charge[28]. Fluorescence can also be quenched due to fluorescence resonance energy transfer (FRET) between the CPEs and molecules with absorption spectra overlapping the polyelectrolyte emission spectrum[18, 29-31]. In a previous work, it was shown that p-nitrophenol (PNP), an electron acceptor that absorbs at 400 nm in its anionic form, is able to quench the fluorescence intensity of blue-emitter cationic polyfluorenes, such as poly{(9,9-bis(6′-N,N,N-trimethylammonium)hexyl]fluorene-phenylene}bromide (HTMA-PFP), presumably via a combination of PET and FRET mechansims[32, 33]. Cao, et al. used this property to develop a fluorimetric assay in buffer for the screening of α-glucosidase inhibitors, exploiting that this enzyme catalyzes the hydrolysis of p-nitrophenyl-α-$_D$-glucopyranoside to PNP. PNP is also the end product of hydrolysis of PNPP, catalyzed by ALP. Therefore, a fluorescent ALP biosensor could be developed by coupling of the polyelectrolyte HTMA-PFP to this enzyme. At a constant concentration of PNPP, this biosensor should be capable of detecting the ALP activity in absence and presence of inhibitors.

The fluorescence quenching of HTMA-PFP and similar polyfluorenes has been also used as a tool to determine DNA, metal-organic ions or proteins in water[34-37]. However, our group reported in a previous study that this polyelectrolyte is not stable in aqueous

solvents[38]. In that work, the photophysical properties of HTMA-PFP were explored in buffer, and compared to those observed in a good solvent. Addition of the polyelectrolyte to the buffer resulted in a strong decrease in the fluorescence intensity and a red-shift of the emission spectrum, evidencing the formation of polymer aggregates. The average size of these aggregates largely increased through the time, inducing the corresponding decrease in their fluorescence intensity. This behaviour is common to other CPEs and must be taken into account to define the real-world sensing applications of this class of polymers, because the fluorescence decrease can be due not only to the presence of a specific analyte but also to the continuous aggregation process. As a consequence, previous stabilization of the CPE in buffer is usually needed before the development of quenching based-sensor systems.

In the present work, we have incorporated HTMA-PFP in lipid vesicles to obtain stable fluorescent nanoparticles (NPs). NPs were characterized and the ability to be quenched by anionic PNP (at alkaline pH) was evaluated. These nanoparticles were coupled to ALP and entrapped in a sol–gel matrix to develop a biosensor that can serve as a screening platform to identify ALP inhibitors. The biosensor was examined before and after the sol-gel entrapment of its components and was used to determine phosphate ion, a competitive inhibitor of ALP. Determination of this analyte is very important in clinical and environmental studies since variations in its optimal concentrations are associated to different pathologies and to the quality of water[39]. The scheme and working principle of the biosensor is shown in Scheme 1.

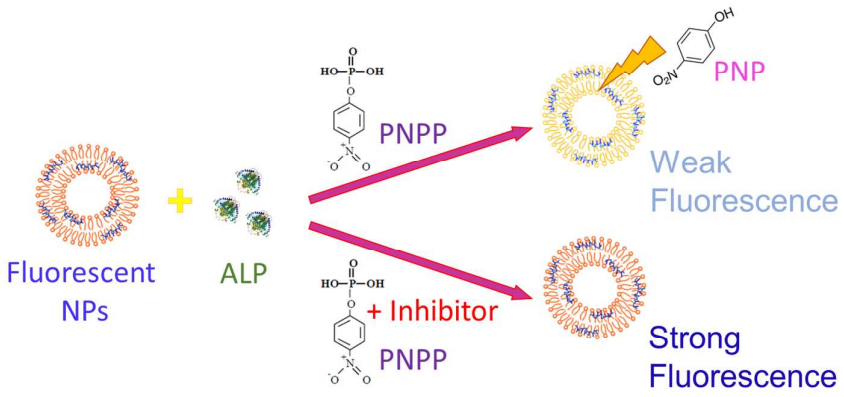

Scheme 1. Working principle of the biosensor: The PNP produced after hydrolysis of PNPP, catalyzed by ALP, quenches the fluorescence of NPs, leading to fluorescence turn-off. The presence of inhibitors inactive the ALP and the fluorescence of the system is preserved.

MATERIALS AND METHODS

The synthetic phospholipid 1,2-Diacyl-sn-glycero-3-phospho-(1-rac-glycerol) (PG), enzyme alkaline phosphatase (ALP) (E.C. 3.1.3.1; from bovine intestinal mucosa, 2982 U/mL), substrate p-nitrophenyl phosphate (PNPP) and the quencher p-nitrophenol (PNP) were obtained from Sigma-Aldrich (St. Louis, MO, USA) and used as received. Stock solutions of ALP, PNPP and PNP were dissolved in Tris buffer (50 mM, pH 9.2) at 40 U/mL, 1.2 mM and 5 mM respectively. Tetraethyl orthosilicate (TEOS) was obtained from Sigma-Aldrich (Spain). All other solvents were of spectroscopic reagent grade (UVASOL, Merck). Tris buffer (50 mM, pH 9.2) was prepared with twice distilled and deionized water, utilizing Milli-Q equipment (Millipore, Madrid, Spain). Enzyme inhibitor, sodium phosphate dibasic (Na_2HPO_4) was purchased from Sigma-Aldrich (Spain). Stock solution of Na_2HPO_4 was prepared with Milli-Q water at 200 mM.

Preparation of the Cationic Polyelectrolyte HTMA-PFP

The polyelectrolyte HTMA-PFP (M = 8340 g/mol, repeat unit molecular weight, M_u= 694,71 g/mol; n'=12) was synthesized in the laboratory from the neutral polymer poly[bis(6´-bromohexyl)fluorene-phenylene], as was previously described[40, 41]. Stock solutions of HTMA-PFP were prepared in DMSO, with final concentrations of 3.65×10^{-4} M (in repeat units) and stored at -20 ºC before use.

Formation of PG Liposomes

To prepare multilamellar vesicles (MLVs), solutions of chloroform/methanol containing 3 mg of PG were dried under nitrogen followed by high vacuum for 3 h. The dried lipid was suspended in the buffer to the required final concentrations (0.5 mM) and vortexed several times. Large unilamellar vesicles (LUVs) were formed by extruding the multilamellar suspension through 100 nm polycarbonate filters (Nucleopore, Cambridge, MA, USA).

Preparation of Fluorescent NPs

Aliquots of HTMA-PFP from the stock solution were added to the LUVs suspension (final concentration of 1.5 μM in terms of repeat units) and incubated during 2 min at room temperature. The proportion of DMSO in the sample was lower than 1% (V/V).

Preparation of the ALP Biosensor in Solution

The ALP biosensor was prepared from the addition of the enzyme ALP stock solution (40 U/mL) to the solution of fluorescent NPs (0.5 mM in lipid). The final enzyme concentration in the sample was 2 U/mL. This value was selected in a previous experiment where the absorbance of the product PNP was measured at 405 nm as a

function of time, using a constant concentration of PNPP (60 μM) (Figure S1). For 2 U/mL of protein, the time needed to hydrolyze the substrate was ~2.5 minutes, which was considered a good response time for the development of the biosensor in solution. For lower concentrations, this time clearly increased up to 6 minutes for 1 U/mL and ~10 minutes for 0.5 U/mL.

Sol-Gel Immobilization of the Fluorescent NPs

Fluorescent NPs were immobilized by the sol-gel process as is described in Martínez-Tomé et al.[42]. A volume of 4.46 mL of the precursor TEOS was mixed at room temperature with 1.44 mL of H_2O and 0.04 mL of HCl (0.62 M). After stirring for one hour, 1 mL of this solution was mixed with 1 mL of distilled water, and submitted to rotaevaporation to eliminate the alcohol resulting from alkoxyde hydrolysis. Immobilized fluorescent nanoparticles were prepared by adding 0.7 mL of the fluorescent NPs to 0.7 mL of the rota-evaporated sample. Transparent monoliths containing the NPs within their pores were rapidly obtained, aged in 0.5 mL of Tris buffer during 24 h and stored at 4ºC in the dark before use. Immobilization of PG liposomes (in the absence of HTMA-PFP) was required as a control for the dispersity of the samples.

Sol-Gel Immobilization of the Enzyme ALP

ALP was immobilized following the same protocol as described above, by adding 0.7 mL of buffered ALP (300 U/mL) solution to 0.7 mL of the rota-evaporated sample. The freshly formed monoliths containing ALP were rinsed with Tris buffer solution and were stored at 4ºC in the dark before use.

Preparation of the ALP Biosensor in Sol-Gel matrix

Solutions containing fluorescent nanoparticles and enzyme ALP were simultaneously immobilized in a sol-gel matrix. In brief, 0.7 mL of a solution containing NPs (PG:HTMA-PFP, 1 mM:3 μM) and ALP (4 U/mL) in Tris buffer were mixed with 0. 7 mL of the rota-evaporated solution. Following gelation, transparent monoliths were obtained, washed with Tris buffer, sealed with parafilm and kept in dark at 4ºC temperature before use.

Fluorescence Measurements

Fluorescence measurements were carried out on a QuantaMaster spectrofluorometer (PTI, Birmingham, NJ, USA) using 1 cm x 1cm path length quartz cuvettes. Samples were excited at 380 nm. Background intensities were subtracted from the sample.

Dynamic Light Scattering (DLS)

Nanoparticles size was estimated by DLS techniques, using a Brookhaven 90 Plus Nanoparticle Size Analyzer instrument equipped with a 35 mW red diode laser (λ = 640 nm) as light source, with a 90° scattering angle of lecture. All measurements were carried out by triplicate using disposable cuvettes.

Transmision Electronic Microscopy (TEM)

TEM was performed using a JEOL JEM-1011 (JEOL, Japan) electron microscope operating at 80kV. Images of polymer aggregates, LUVs and NPs were obtained by placing a drop of the corresponding suspension onto copper grids (300 mesh) coated with carbon film, and then stained with lead citrate and uranyl acetate. These samples

were left to air-dry before being placed under the microscope. Digital images were recorded with a Gatan Erlangshen ES500W camera.

RESULTS AND DISCUSSION

Design of Fluorescent Nanoparticles (NPs)

As was mentioned in the Introduction, HTMA-PFP and, in general, CPEs have high tendency to aggregate in aqueous environment leading to detrimental emission quenching. Several methods are being developed to stabilize and increase the quantum yield of the CPEs by overcoming the aggregation[43]. In the present work, stabilization of the HTMA-PFP was obtained through the incorporation of the polyelectrolyte in LUVs, using the same strategy previously reported by our group for the stabilization of other polyfluorenes[44]. We selected phosphatidylglycerol (PG) lipid vesicles due to the high affinity of HTMA-PFP for anionic vesicles and its insertion in the hydrophobic core of the lipid bilayer[38, 45]. Vesicles were prepared in Tris buffer, pH 9.2, which is an adequate pH for ALP activity. The lipid concentration was fixed to 0.5 mM to limit the turbidity of samples which becomes an obstacle for fluorescence measurements. The polymer concentration was 1.5 μM to ensure that all the polymer chains were incorporated in the vesicles, taking into account its partition coefficient between lipid and aqueous phase. In addition, the integrity of the vesicle was preserved at this polymer concentration[38]. Figure 1 shows the emission spectra and the stability plot obtained at these conditions for HTMA-PFP in PG and Tris buffer. The low fluorescence intensity (Figure 1a) and its decrease as a function of time (Figure 1c) confirm the formation of aggregates of polyelectrolyte in buffer. The incorporation of the HTMA-PFP into the vesicles is evidenced by the increase of the fluorescence

intensity and the blue shift of the fluorescence spectrum when compared to the buffer (Figures 1a-b). This behavior is probably due to the transformation of the initially formed polymer aggregates into liposomal nanoparticles (NPs) within which polymer segments are separated by the lipid molecules. The fact that the fluorescence intensity was constant as a function of time confirms the total incorporation of the polymer chains in the vesicles (Figure 1c).

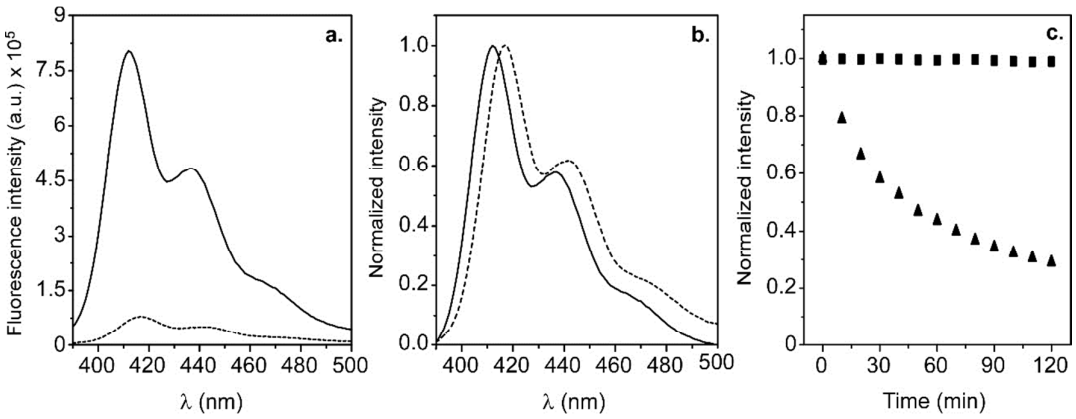

Figure 1. a) Fluorescence emission spectra and **b)** Normalized fluorescence emission spectra of HTMA-PFP in LUVs of PG (solid) and Tris buffer pH 9.2 (dash). **c)** Normalized fluorescence intensity at the maximum emission wavelength of HTMA-PFP in LUVs of PG (squares) and Tris buffer pH 9.2 (triangles) recorded as a function of time. (λ_{exc}=380 nm).

The formed NPs were furtherly characterized by DLS. This technique was used to confirm their formation as well as to check their size and stability through time. The hydrodynamic radius (Rh) of the vesicles was measured before and after the addition of HTMA-PFP and was compared to that obtained for the polyelectrolyte in the Tris buffer. Results obtained in the buffer solution confirm the formation of aggregates and their instability through time (Table 1). For the vesicles, in absence of HTMA-PFP, a single distribution was observed with Rh ~ 86 nm. When the polyelectrolyte was incorporated into the vesicles to form the fluorescent NPs, a similar distribution

centered at 89 nm was obtained and no additional population was detected. The DLS results support that HTMA-PFP is well inserted in the lipid bilayer because the vesicle size is not changing after polymer interaction. The fact that the same result was obtained 1 h after the preparation confirms that aggregates of HTMA-PFP are not present in the buffer, thus all the polymer chains are forming NPs. In addition, it supports that the integrity of the lipid vesicles is maintained after polyelectrolyte incorporation since we have not observed any vesicle fusion or decomposition into small fragments. These nanoparticles remained stable even 24h after preparation as can be inferred from the Rh values measured during this time period (Table 1). The above results were also supported by TEM experiments. Images of polymer aggregates and lipid vesicles in absence and presence of the polymer are shown in Figure S2, Supporting Information. Results are in agreement with those obtained in DLS experiments and show that the polyelectrolyte does not alter the integrity, size and morphology of the vesicles and that vesicle fusion is not taking place.

Sample	Rh **(nm)**		
	t_0	$t = t_0 + 1h$	$t = t_0 + 24h$
PG LUVs	86	89	89
NPs	89	89	88
HTMA-PFP/Buffer	85	130	180

Table 1. Average hydrodynamic radii, Rh, determined by DLS measurements for different samples: PG LUVs, NPs (HTMA-PFP/PG LUVs) and HTMA-PFP in Tris buffer pH 9.2, recorded at different times after preparation.

Once the stability of the fluorescent NPs was confirmed, the ability to be quenched by PNP was explored as an essential requirement for the biosensor construction. Increasing concentrations of PNP (0 to 20 μM) were added to a suspension of NPs and their emission spectra were recorded after each addition. A decrease in the fluorescence intensity was observed as the quencher concentration was increased (Figure 2). This result indicates that, in spite of HTMA-PFP is incorporated into the vesicles and, therefore, much less accessible to the water-soluble PNP, its fluorescence still can be quenched. This behaviour supports that in addition to PET, FRET is also one of the quenching mechanisms of HTMA-PFP by PNP, because at difference of PET, which occurs efficiently only upon van der Waals contact between fluorophore and quencher, the FRET process takes place over much longer distances (2-10 nm). The inset of Figure 2 shows that the dependence of the fluorescence intensity on the quencher concentration is linear, being described by a Stern-Volmer plot with a value of $K_{SV}=5.08\pm0.07x10^{4}$ M^{-1}. This value is large but about 7-fold lower than the value reported for the same polyelectrolyte in buffer[32]. A decrease in the quenching efficiency has been also reported for other CPEs in presence of surfactants[46, 47], and reflects a lower association constant between quencher and polymer. In our case, the decrease in K_{SV} can be attributed to two factors, both of which reduce the electron transfer probability between HTMA-PFP and PNP: firstly, the previously mentioned lower accessibility of the PNP to the polyelectrolyte, which is inserted in the bilayer; secondly, a reduction in the electrostatic attraction between PNP and HTMA-PFP, because the polyelectrolyte cationic charge is partially neutralized by interactions with the anionic lipid heads. In addition, the high quenching efficiency reported for the HTMA-PFP in buffer could be also overestimated because of the continuous

aggregation process, previously described, which largely decreases the fluorescence intensity due to self-quenching.

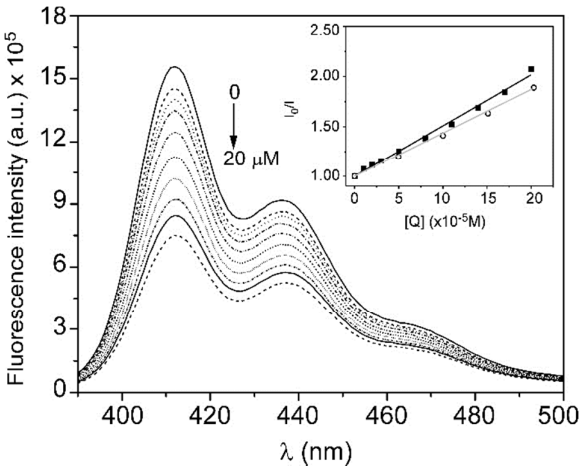

Figure 2. Fluorescence emission spectra of NPs at increasing concentrations of PNP. Inset: Stern-Volmer plots for quenching of NPs by PNP (black squares) and after addition of PNPP (60μM) to NPs, in presence of ALP (2 U/mL) (circles).

Development of the ALP Biosensor: Study in Solution

Once proved the quenching of the fluorescent nanoparticles by PNP, we investigated their ability to detect ALP activity, taking into account that this enzyme catalyses the hydrolysis of PNPP to PNP. With this end, firstly we recorded the emission spectra of the NPs in absence and presence of ALP (2 U/mL), and the areas under the spectra were plotted in Figure 3a. The fact that this area was not affected by the presence of the enzyme suggests that no interaction is occurring between them. However, the addition of substrate PNPP (60 μM) to the sample containing the enzyme induced a strong decrease in the fluorescence intensity of the NPs which was monitored as a function of time (Figure 3b). The fluorescence intensity practically reached its minimum value (~ 12 % of the initial value) in the 2 first min after addition of substrate, reflecting the

kinetics of the enzymatic activity. To confirm that the fluorescence quenching was due to the PNP formed from the hydrolysis of PNPP, increasing concentrations of substrate (0 to 20 μM) were added to a sample containing NPs and ALP. Fluorescence spectra were recorded after 3 min of incubation for each substrate concentration. The inset of Figure 2 shows the SternVolmer plot corresponding to this experiment. The Stern-Volmer constant extracted from the lineal plot (K_{SV}=4.94±0.28x10^4 M^{-1}) was very close to that obtained when PNP was directly added to the NPs suspension, evidencing the adequate operation of the biosensor in solution.

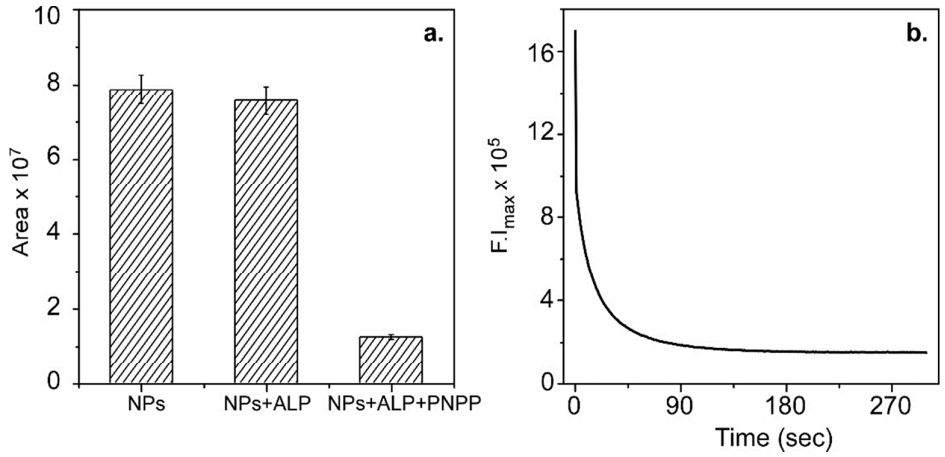

Figure 3. a) Fluorescence intensities represented as integrated areas under the emission spectrum, for the fluorescent NPs without and with ALP (2 U/mL) and in presence of ALP and PNPP (60 μM), after 3 min of incubation. **b)** Fluorescence intensity kinetics of NPs in presence of ALP (2 U/mL), recorded after addition of PNPP (60 μM). (λ_{exc}=380 nm ; λ_{em}=412 nm).

As was described in the Introduction, this biosensor could be used for ALP inhibitors screening and to determine the concentration of a specific inhibitor in a sample. The mechanism of sensing is shown in Scheme 1 and is based on the fluorescence turn-off/turn on. The PNP produced after hydrolysis of PNPP quenches the fluorescence of NPs, leading to fluorescence turn-off. The presence of inhibitors prevents this effect and

a higher fluorescence signal is observed compared to that recorded in absence of inhibitors. This potential application was explored using phosphate ion, which is a competitive inhibitor of the enzyme. To carry out this study different samples containing the fluorescent NPs in presence of ALP (2 U/mL) and increasing concentrations of phosphate ion (0 to 1 mM) were prepared. The same concentration of PNPP (60 μM) was added to all the samples and the quenching of fluorescence (which reflects the ALP activity) was recorded as a function of time for each sample. The quenching kinetics was found to be slower as the concentration of phosphate increases, evidencing a significant decrement in the enzymatic activity (Figure 4a). This result indicates that our method is sensitive to the presence of the phosphate ions and therefore, it could be used for the determination of inhibitors. Results are shown in Figure 4b in form of calibration curve. The plot represents the maximum fluorescence intensity of the NPs, recorded 3 minutes after PNPP addition, *versus* phosphate ion concentration. This plot was linear in the range of concentrations studied (up to 1 mM), with a limit of detection (LOD) of 52 μM, equivalent to three times the blank value[48]. This LOD is lower than the concentration of phosphate which is normally present in human blood serum (1.1-1.4 mM) and is similar to that recently reported for an ALP-conductimetric biosensor[49].

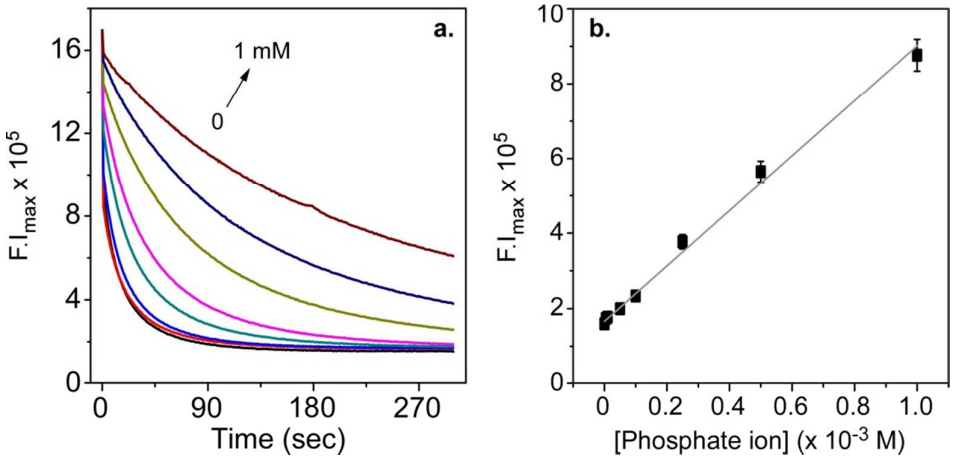

Figure 4. a) Time-dependent fluorescence intensity of NPs, in presence of ALP (2 U/mL) and increasing concentrations of phosphate ions, after addition of PNPP (60 μM). **b)** Phosphate ion calibration curve. The fluorescence intensities were taken 3 minutes after the addition of PNPP to each sample. (λ_{exc}=380 nm ; λ_{em}=412 nm).

Development of the ALP Biosensor: Immobilization of Components

The practical application of the biosensor described above requires the preparation of different samples (fluorescent NPs, fresh solutions of the enzyme, etc.) for each use, with the consequent time and economic burden. Immobilization of the biosensor components would facilitate their handling, enabling their reutilization and thus reducing the cost of the procedure. In the last two decades, the renaissance of sol–gel chemistry has provided a versatile methodology for the immobilization and stabilization of numerous biological systems, such as enzymes and liposomes, in transparent inorganic glasses[50-56]. Sol–gel immobilization has many advantages over other immobilization methods, including encapsulation of large amount of biomolecules, chemical and thermal stability of the sol-gel glasses, enhanced stability of the entrapped macromolecules and flexibility in controlling geometry and pore size. In addition, thanks to the porous nature of the material, the entrapped biomolecules remain

accessible to specific analytes, with negligible macromolecule leaching. In this work, we have selected the sol-gel methodology to simultaneously encapsulate the biosensor components: ALP and NPs in the pores of a single matrix to obtain a stable, easy-to-use and reusable device for detection of ALP inhibitors. Firstly, each component of the biosensor was immobilized separately, to check the effects of the immobilization process on its properties, as is described below.

A preliminary analysis was done to demonstrate that the immobilization process did not affect the fluorescent properties of NPs. Fluorescence spectra of the immobilized NPs were directly measured from the monolith and are shown in the inset of Figure 5a. The shape and spectral position, as well as the fluorescence intensity, were very similar to those observed for the spectrum of NPs in buffer, suggesting the suitability of the immobilization method.

To better characterize the immobilized NPs, we explored their stability by monitoring the fluorescence spectra as a function of time, pH and temperature. Figure 5a and its inset show the effect of storage time (up to 12 days) on the fluorescence intensity of the NPs, as well as on the shape and position of the emission spectrum. All these parameters were not affected during this period of time. Larger stability (up to 6 months) was also found when the monolith was kept at 4ºC protected from light (data not shown). These results indicate that the immobilized NPs are chemically and physically stable and that the leaching of the nanoparticles from the sol-gel monolith is very limited or negligible during, at least, six months.

The effect of pH on the stability of the immobilized NPs was explored by immersion of the monoliths in aqueous samples at different pHs (from pH 2.5 to pH 10.5) for 30 minutes before measurements. Fig. 5b shows the normalized fluorescence intensity recorded from these monoliths, together with their emission spectrum (inset in Figure

5b). Results show that the incorporation of the monolith in an acidic or basic solution does not alter the intensity, shape and spectral position of the immobilized NPs, suggesting that they are stable under these conditions.

Finally, thermal stability was explored measuring the emission spectrum of the immobilized NPs between 15 and 55ºC (Figure 5c). The increase of temperature caused a small decrease in the fluorescence intensity as well as a slight blue shift of the spectrum, followed by a decrease in the spectral resolution. Similar changes have been described for other conjugated polymers[42, 44, 57] and suggest an increase in the degrees of freedom of the polyelectrolyte within the lipid bilayer (inset in Figure 5c). When the monolith was cooled to 25ºC, the initial fluorescence spectrum was recovered. This result indicates that the reduction of intensity is mainly caused by the increase of probability of nonradiative transitions at higher temperatures, and not by degradation of NPs. The high stability of the sol-gel immobilized NPs under different conditions open the possibility of using this system not only for the ALP biosensor, but also for the development of many other sensing applications.

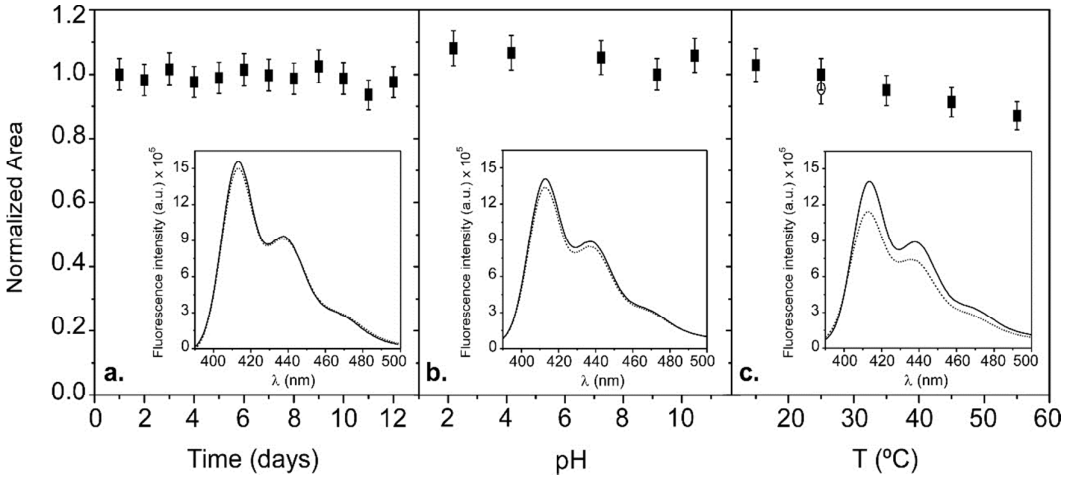

Figure 5. Stability of the immobilized NPs as a function of storage time (**a**), pH (**b**) and temperature (**c**), measured as the area under the fluorescence spectrum. Inset: Effect of time (**a**), pH (**b**) and temperature (**c**) on the fluorescent emission spectra of the immobilized NPs For temperature experiments the sample was heated from 15 to 55 ºC (squares) and subsequently cooled to room temperature (circle). (λ_{exc}=380nm).

Once the stability of the immobilized NPs was ensured, we investigated the possibility of being quenched by PNP. With this end, a monolith containing NPs was introduced in a PNP solution (200 μM) and the fluorescence spectrum of the monolith was recorded as a function of time. Contrary to that found for free NPs in solution, no intensity decrease was observed in the first seconds, and longer time was required to quench the fluorescence of NPs (Figure 6a). This result confirms that the immobilized NPs can be still quenched by PNP but indicates that PNP diffuses much more slowly through matrix than through the buffer. This behaviour has been observed for other analytes and is attributed to the steric restrictions imposed by the sol-gel matrix[50]. The same experiment was carried out with other two monoliths in order to explore the reproducibility of the assay. A similar quenching kinetics was obtained for the three monoliths confirming that the behaviour of the NPs immobilized in the sol-gel matrices is highly reproducible (Figure 6a).

The suitability of the encapsulated NPs to be quenched by PNP was confirmed above. In the following step, we explored the capability of reusing the above monoliths after the elimination of PNP by washing. With this end, monoliths were immersed in Tris buffer every 1 hour for 3 times. Figure 6b shows the quenching kinetics recorded for one of these monoliths before and after washing with buffer. Both curves were very similar confirming the possibility to use the same monolith in more than one occasion without losing efficacy.

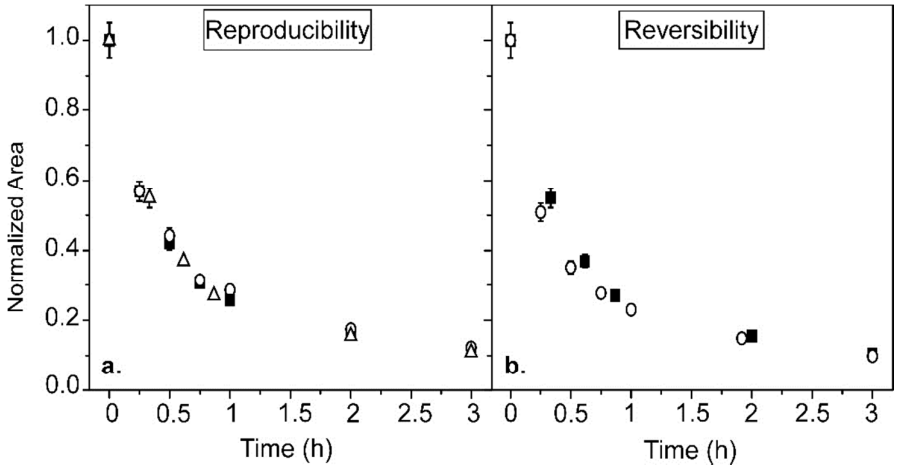

Figure 6. Fluorescence quenching kinetics of immobilized NPs after addition of PNP: **a)** Reproducibility of the assay using three different monoliths; **b)** Reutilization of the monoliths: first (squares) and second (circles) use.

As for immobilized NPs, a preliminary experiment was performed to check the effects of sol-gel encapsulation on the properties of ALP, by following changes in its intrinsic fluorescence (mainly from tryptophan). The fluorescence of tryptophan is very sensitive to the polarity of its environment, providing a convenient probe to distinguish native and unfolded states of proteins. To obtain fluorescence spectra of good quality the concentration of the free and immobilized protein was increased to 150 U/mL, due to its low fluorescence quantum yield. Figure 7 shows the emission spectra recorded in solution and after the sol-gel immobilization. The similarity between both spectra indicates the suitability of the immobilization method.

After ALP was successfully encapsulated in the sol-gel matrix, the kinetic properties of the protein were tested by immersion of the monolith in a solution containing PNPP and fluorescent NPs. Note that for this study, the protein concentration in the matrix was 2 U/mL, as for the assay in solution. Emission spectra, recorded from the solution, were

taken each 10 minutes. Inset in Figure 7 shows the decrease of the fluorescence intensity as a function of the incubation time.

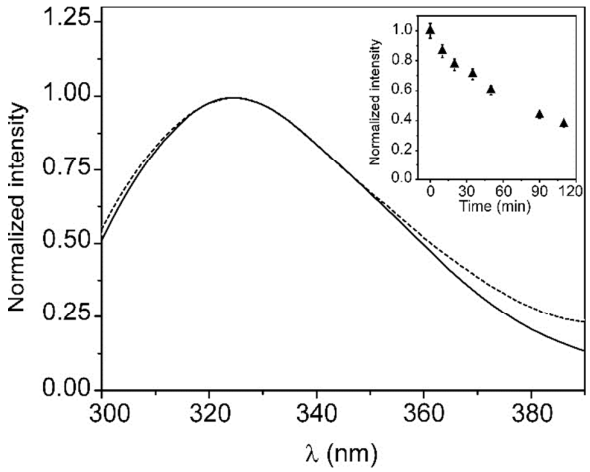

Figure 7. Fluorescence emission spectra of free (solid) and immobilized (dash) ALP (150 U/mL) (λ_{exc}=290 nm). **Inset:** Fluorescence intensity kinetics of NPs measured in a PNPP solution (60 μM), after immersion of the protein-containing matrix (2 U/mL).

The fluorescence decrease confirms the formation of PNP and, therefore, the functioning of the enzyme. However, the kinetics was largely slower than that obtained for the enzyme in solution. As was discussed for the immobilized NPs, this result suggests that diffusion of PNP and PNPP through the matrix is restricted, limiting the response time of the sol-gel biosensor. A similar result was obtained by García Sánchez et al. when ALP was entrapped in a sol-gel matrix to obtain a biosensor for the determination of pesticides[58].

Alkaline Phosphatase Biosensor in Sol-Gel Matrices.

The above results indicate the suitability of the immobilization methodology for the components separately and suggest that the slow diffusion of PNPP and PNP through the sol-gel matrix slows down the fluorescence quenching. The following step was the co-immobilization of both NPs and ALP in the same sol-gel monolith to obtain the final form of the biosensor. This monolith was immersed in a solution containing PNPP and its fluorescence was measured at different incubation times. To reduce the response time of the biosensor due to diffusional restrictions, the concentration of substrate was increased from 0.6 μM to 0.2 and 1 mM. Figure 8a shows the results of this experiment. The fluorescence decrease confirms the formation of PNP and, therefore, the suitability of the co-immobilization process. Increasing the PNPP concentration resulted in a clear improvement of the assay. Using 1 mM of substrate, a 90% of quenching was obtained after 30 minutes of incubation (Figure 8a), which is an acceptable time of response for a biosensor. These conditions were selected to check the possible reutilization of the biosensor. The same monolith was used for seven consecutive assays and the efficiency of the quenching was measured after 30 minutes of incubation (Figure 8b). After each assay, the monolith was washed with Tris buffer for 3 h by changing the buffer every hour to remove the residual PNP. The fact that the quenching efficiency is similar in all the assays demonstrates that this biosensor can be used repeatedly for various measurements without losing its sensitivity.

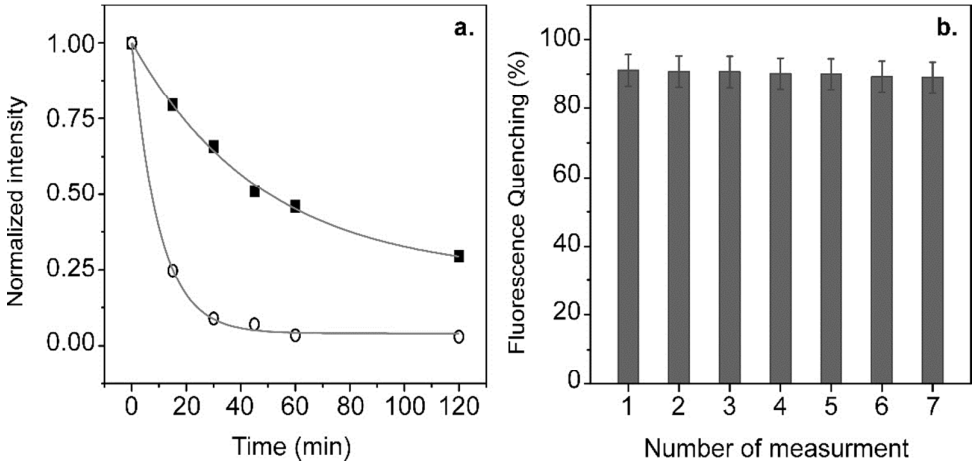

Figure 8. a) Fluorescence quenching kinetics measured in the immobilized biosensor after its immersion in a solution containing 200 μM PNPP (black squares) and 1 mM PNPP (circles). **b)** Reusability study of the biosensor performed using the same monolith after washing with buffer, for seven consecutive assays, measuring the fluorescence quenching percentage after 30 minutes of incubation ([PNPP]=1mM).

Once the working conditions of the biosensor were optimized, we explored its ability to determine the presence of inhibitors such as phosphate ion. Figure 9a shows the fluorescence quenching percentage obtained in absence and presence of 1mM of phosphate ion, after 30 min of incubation. The drop in the quenching efficiency confirms the capacity of the biosensor to detect the inhibitor. Results are shown in Figure 9b in the form of calibration curve. To build this curve, the biosensor was immersed in buffer samples containing increasing concentrations of phosphate ion (0 to 5 mM). After the addition of 1mM PNPP, monoliths were incubated for 30 min and then their fluorescence intensity was measured and plotted as a function of phosphate concentration. This plot was linear in the range of concentrations studied (up to 5 mM), with a limit of detection (LOD) of 370 μM, equivalent to three times the blank value. This biosensor shows a LOD higher than that obtained in solution, but still lower than

the concentration of phosphate normally present in human blood serum (1.1-1.4 mM), having the advantage of being reusable.

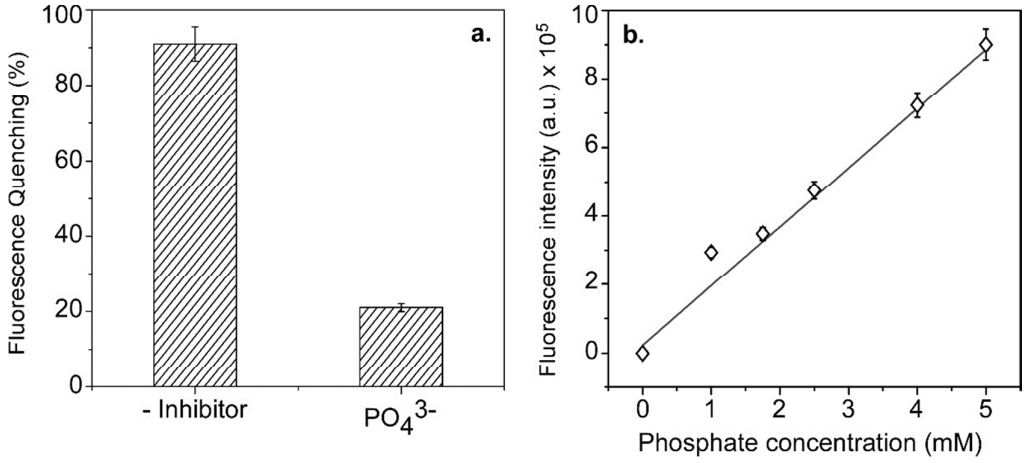

Figure 9. a) Percentage of fluorescence quenching, after the addition of PNPP (1mM) to the immobilized ALP biosensor, in the absence of inhibitor compared to that obtained in the presence of inhibitor phosphate ion (5mM). **b)** Fluorescence intensities recorded for immobilized ALP biosensor in the absence and presence of different concentrations of phosphate ions.

CONCLUSIONS

In this work, we have developed a fluorescent biosensor for the detection of phosphate ion, a competitive inhibitor of the enzyme ALP. The biosensor is based on the fluorescence intensity quenching of the conjugated polyelectrolyte HTMA-PFP induced by PNP, the hydrolysis product of PNPP being catalysed by the ALP. HTMA-PFP was previously stabilized in buffer through its interaction with lipid vesicles to obtain blue-emitting nanoparticles (NPs). These NPs were stable under pH and temperature and their fluorescence was efficiently quenched by PNP. The coupling of NPs with ALP in solution was used to develop a biosensor able to rapidly determine the concentration of

ion phosphate in an aqueous sample with a LOD of 52 μM. In order to improve the performance of the biosensor, its components (NPs and ALP) were immobilized in a sol-gel matrix, making the biosensor reusable for, at least, seven assays. The device was successfully used for the determination of phosphate ion, with a LOD higher than the one determined in the solution, and a longer response time that reflects the slower diffusion of PNPP and PNP through the matrix. This methodology could be easily extrapolated for the screening of inhibitors of other enzymes, such as α-glucosidase and α-galactosidase, which catalyze reactions yielding PNP as final product.

SUPPORTING INFORMATION:

Optimization of the enzyme concentration and TEM experiments are included in the Supporting information as Figures S1 and S2. This material is available free of charge via the Internet at http://pubs.acs.org.

AUTHOR INFORMATION

Corresponding Author

*E-mail: rmateo@umh.es

ACKNOWLEDGMENTS

This work was supported by grants from the Spanish Ministerio de Economia y Competitividad (MAT-2014-53282-R) and Generalitat Valenciana (PROMETEO/2013/018).

References

(1) Alvarado-Gámez, A. L.; Alonso-Lomillo, M. A.; Domínguez-Renedo, O.; Arcos-Martínez, M. J. A Disposable Alkaline Phosphatase-Based Biosensor for Vanadium Chronoamperometric Determination. *Sensors* **2014**, *14*, 3756-3767.

(2) Miao, P.; Ning, L.; Li, X.; Shu, Y.; Li, G. An Electrochemical Alkaline Phosphatase Biosensor Fabricated with Two DNA Probes Coupled with Λ Exonuclease. *Biosens. Bioelectron.* **2011**, *27*, 178-182.

(3) Mousty, C.; Kaftan, O.; Prevot, V.; Forano, C. Alkaline Phosphatase Biosensors Based on Layered Double Hydroxides Matrices: Role of LDH Composition. *Sens. Actuators, B* **2008**, *133*, 442-448.

(4) Neagu, D.; Micheli, L.; Palleschi, G. Study of a Toxin-Alkaline Phosphatase Conjugate for the Development of an Immunosensor for Tetrodotoxin Determination. *Anal. Bioanal. Chem.* **2006**, *385*, 1068-1074.

(5) Yin, Z.; Liu, Y.; Jiang, L. P.; Zhu, J. J. Electrochemical Immunosensor of Tumor Necrosis Factor a Based on Alkaline Phosphatase Functionalized Nanospheres. *Biosens. Bioelectron.* **2011**, *26*, 1890-1894.

(6) Wang, S.; Su, P.; Huang, J.; Wu, J.; Yang, Y. Magnetic Nanoparticles Coated with Immobilized Alkaline Phosphatase for Enzymolysis and Enzyme Inhibition Assays. *J. Mater. Chem. B* **2013**, *1*, 1749-1754.

(7) Qian, Z. S.; Chai, L. J.; Huang, Y. Y.; Tang, C.; Jia Shen, J.; Chen, J. R.; Feng, H. A Real-Time Fluorescent Assay for the Detection of Alkaline Phosphatase Activity Based on Carbon Quantum Dots. *Biosens. Bioelectron.* **2015**, *68*, 675-680.

(8) Liu, S.; Pang, S.; Na, W.; Su, X. Near-Infrared Fluorescence Probe for the Determination of Alkaline Phosphatase. *Biosens. Bioelectron.* **2014**, *55*, 249-254.

(9) Deng, J.; Yu, P.; Wang, Y.; Mao, L. Real-Time Ratiometric Fluorescent Assay for Alkaline Phosphatase Activity with Stimulus Responsive Infinite Coordination Polymer Nanoparticles. *Anal. Chem.* **2015**, *87*, 3080-3086.

(10) Duarte, A.; Pu, K. Y.; Liu, B.; Bazan, G. C. Recent Advances in Conjugated Polyelectrolytes for Emerging Optoelectronic Applications. *Chem. Mater.* **2011**, *23*, 501-515.

(11) Houston, J. E.; Kraft, M.; Scherf, U.; Evans, R. C. Sequential Detection of Multiple Phase Transitions in Model Biological Membranes using a Red-Emitting Conjugated Polyelectrolyte. *Phys. Chem. Chem. Phys.* **2016**, *18*, 12423-12427.

(12) Houston, J. E.; Kraft, M.; Mooney, I.; Terry, A. E.; Scherf, U.; Evans, R. C. Charge-Mediated Localization of Conjugated Polythiophenes in Zwitterionic Model Cell Membranes. *Langmuir* **2016**, *32*, 8141-8153.

(13) Thomas III, S. W.; Joly, G. D.; Swager, T. M. Chemical Sensors Based on Amplifying Fluorescent Conjugated Polymers. *Chem. Rev.* **2007**, *107*, 1339-1386.

(14) Pu, K. Y.; Cai, L.; Liu, B. Design and Synthesis of Charge-Transfer-Based Conjugated Polyelectrolytes as Multicolor Light-Up Probes. *Macromolecules* **2009**, *42*, 5933-5940.

(15) Jiang, H.; Taranekar, P.; Reynolds, J. R.; Schanze, K. S. Conjugated Polyelectrolytes: Synthesis, Photophysics, and Applications. *Angew. Chem. Int. Ed.* **2009**, *48*, 4300-4316.

(16) Kim, S.; Lim, C. K.; Na, J.; Lee, Y. D.; Kim, K.; Choi, K.; Leary, J. F.; Kwon, I. C. Conjugated Polymer Nanoparticles for Biomedical in Vivo Imaging. *Chem. Commun.* **2010**, *46*, 1617-1619.

(17) Smith, B. A.; Smith, B. D. Biomarkers and Molecular Probes for Cell Death Imaging and Targeted Therapeutics. *Bioconjugate Chem.* **2012**, *23*, 1989-2006.

(18) Zhu, C.; Liu, L.; Yang, Q.; Lv, F.; Wang, S. Water-Soluble Conjugated Polymers for Imaging, Diagnosis, and Therapy. *Chem. Rev.* **2012**, *112*, 4687-4735.

(19) Feng, L.; Zhu, C.; Yuan, H.; Liu, L.; Lv, F.; Wang, S. Conjugated Polymer Nanoparticles: Preparation, Properties, Functionalization and Biological Applications. *Chem. Soc. Rev.* **2013**, *42*, 6620-6633.

(20) Lyu, Y.; Xie, C.; Chechetka, S. A.; Miyako, E.; Pu, K. Semiconducting Polymer Nanobioconjugates for Targeted Photothermal Activation of Neurons. *J. Am. Chem. Soc.* **2016**, *138*, 9049-9052.

(21) Miao, Q.; Lyu, Y.; Ding, D.; Pu, K. Semiconducting Oligomer Nanoparticles as an Activatable Photoacoustic Probe with Amplified Brightness for in Vivo Imaging of pH. *Adv. Mater.* **2016**, *28*, 3662-3668.

(22) Kahveci, Z.; Vázquez-Guilló, R.; Mira, A.; Martinez, L.; Falcó, A.; Mallavia, R.; Mateo, C. R. Selective Recognition and Imaging of Bacterial Model Membranes Over Mammalian Ones by using Cationic Conjugated Polyelectrolytes. *Analyst* **2016**, *141*, 6287-6296.

(23) Ngo, A. T.; Karam, P.; Cosa, G. Conjugated Polyelectrolyte-Lipid Interactions: Opportunities in Biosensing. *Pure Appl. Chem.* **2011**, *83*, 43-55.

(24) Liu, Y.; Ogawa, K.; Schanze, K. S. Conjugated Polyelectrolytes as Fluorescent Sensors. *J. Photochem. Photobiol. ,C* **2009***, 10*, 173-190.

(25) Wang, L.; Li, H.; Cao, D. Conjugated Polyelectrolytes: Synthesis and Application in Biomolecule Detection. *Curr. Org. Chem.* **2012***, 16*, 1468-1484.

(26) Tang, Y.; Liu, Y.; Cao, A. Strategy for Sensor Based on Fluorescence Emission Red Shift of Conjugated Polymers: Applications in pH Response and Enzyme Activity Detection. *Anal. Chem.* **2013***, 85*, 825-830.

(27) Toal, S. J.; Trogler, W. C. Polymer Sensors for Nitroaromatic Explosives Detection. *J. Mater. Chem.* **2006***, 16*, 2871-2883.

(28) Chen, L.; McBranch, D. W.; Wang, H. -.; Helgeson, R.; Wudl, F.; Whitten, D. G. Highly Sensitive Biological and Chemical Sensors Based on Reversible Fluorescence Quenching in a Conjugated Polymer. *Proc. Natl. Acad. Sci. U. S. A.* **1999***, 96*, 12287-12292.

(29) Senthilkumar, T.; Asha, S. K. Selective and Sensitive Sensing of Free Bilirubin in Human Serum using Water-Soluble Polyfluorene as Fluorescent Probe. *Macromolecules* **2015***, 48*, 3449-3461.

(30) Qin, C.; Cheng, Y.; Wang, L.; Jing, X.; Wang, F. Phosphonate-Functionalized Polyfluorene as a Highly Water-Soluble Iron(III) Chemosensor. *Macromolecules* **2008***, 41*, 7798-7804.

(31) Qin, C.; Tong, H.; Wang, L. Water-Soluble Phosphate-Functionalized Polyfluorene as Fluorescence Biosensors Toward Cytochrome C. *Sci. China, Ser. B: Chem.* **2009***, 52*, 833-839.

(32) Cao, A.; Tang, Y.; Liu, Y. Novel Fluorescent Biosensor for a-Glucosidase Inhibitor Screening Based on Cationic Conjugated Polymers. *ACS Appl. Mater. Interfaces* **2012***, 4*, 3773-3778.

(33) Naeem, A.; Khan, I. M.; Ahmad, A. Spectral Investigations of Multiple Charge Transfer Complex of P-Nitrophenol as an Electron Acceptor with Donor P-Dimethylaminobenzaldehyde. *Russ. J. Phys. Chem. A* **2011***, 85*, 1840-1843.

(34) Tapia, M. J.; Montserín, M.; Valente, A. J. M.; Burrows, H. D.; Mallavia, R. Binding of Polynucleotides to Conjugated Polyelectrolytes and its Applications in Sensing. *Adv. Colloid Interface Sci.* **2010***, 158*, 94-107.

(35) Martínez-Tome, M. J.; Esquembre, R.; Mallavia, R.; Mateo, C. R. Formation of Complexes between the Conjugated Polyelectrolyte Poly{[9,9-Bis(6'-N,N,Ntrimethylammonium) Hexyl]Fluorene-Phenylene} Bromide (HTMA-PFP) and Human Serum Albumin. *Biomacromolecules* **2010***, 11*, 1494-1501.

(36) Maiti, J.; Pokhrel, B.; Boruah, R.; Dolui, S. K. Polythiophene Based Fluorescence Sensors for Acids and Metal Ions. *Sens. Actuators, B* **2009***, 141*, 447-451.

(37) Fan, L. -.; Zhang, Y.; Murphy, C. B.; Angell, S. E.; Parker, M. F. L.; Flynn, B. R.; Jones Jr., W. E. Fluorescent Conjugated Polymer Molecular Wire Chemosensors for Transition Metal Ion Recognition and Signaling. *Coord. Chem. Rev.* **2009**, *253*, 410-422.

(38) Kahveci, Z.; Martínez-Tomé, M. J.; Mallavia, R.; Mateo, C. R. Use of the Conjugated Polyelectrolyte Poly{[9,9-Bis(6'- N, N, N-Trimethylammonium)Hexyl]Fluorene-Phenylene} Bromide (HTMA-PFP) as a Fluorescent Membrane Marker. *Biomacromolecules* **2013**, *14*, 1990-1998.

(39) Upadhyay, L. S. B.; Verma, N. Recent Advances in Phosphate Biosensors. *Biotechnol. Lett.* **2015**, *37*, 1335-1345.

(40) Molina, R.; Gómez-Ruiz, S.; Montilla, F.; Salinas-Castillo, A.; Fernández-Arroyo, S.; Del Mar Ramos, M.; Micol, V.; Mallavia, R. Progress in the Synthesis of Poly(2,7-Fluorene-Alt-1,4-Phenylene), PFP, Via Suzuki Coupling. *Macromolecules* **2009**, *42*, 5471-5477.

(41) Mallavia, R.; Martinez-Peréz, D.; Chmelka, B. F.; Bazan, G. C. Blue Fluorescent Films Based on Poly-2,7-Fluorene-Phenylene Derivatives. *Bol. Soc. Esp. Ceram. Vidrio* **2004**, *43*, 327-330.

(42) Martínez-Tomé, M. J.; Esquembre, R.; Mallavia, R.; Mateo, C. R. Formation and Characterization of Stable Fluorescent Complexes between Neutral Conjugated Polymers and Cyclodextrins. *J. Fluoresc.* **2013**, *23*, 171-180.

(43) Al Attar, H. A.; Monkman, A. P. Effect of Surfactant on Water-Soluble Conjugated Polymer used in Biosensor. *J Phys Chem B* **2007**, *111*, 12418-12426.

(44) Kahveci, Z.; Vázquez-Guilló, R.; Martínez-Tomé, M. J.; Mallavia, R.; Mateo, C. R. New Red-Emitting Conjugated Polyelectrolyte: Stabilization by Interaction with Biomolecules and Potential use as Drug Carriers and Bioimaging Probes. *ACS Appl. Mater. Interfaces* **2016**, *8*, 1958-1969.

(45) Kahveci, Z.; Martínez-Tomé, M. J.; Esquembre, R.; Mallavia, R.; Mateo, C. R. Selective Interaction of a Cationic Polyfluorene with Model Lipid Membranes: Anionic Versus Zwitterionic Lipids. *Materials* **2014**, *7*, 2120-2140.

(46) López-Cabarcos, E.; Retama, J. R.; Sholin, V.; Carter, S. A. Controlling the Photoluminescence of Water-Soluble Conjugated Poly[2-(3-Thienyl)Ethyloxy-4-Butylsulfonate)] for Biosensor Applications. *Polym. Int.* **2007**, *56*, 588-592.

(47) Chen, L.; Xu, S.; McBranc, D.; Whitten, D. Tuning the Properties of Conjugated Polyelectrolytes through Surfactant Complexation [4]. *J. Am. Chem. Soc.* **2000**, *122*, 9302-9303.

(48) Thomsen, V.; Schatzlein, D.; Mercuro, D. Limits of Detection in Spectroscopy. *Spectroscopy* **2003**, *18*, 112-114.

(49) Upadhyay, L. S. B.; Verma, N. Alkaline Phosphatase Inhibition Based Conductometric Biosensor for Phosphate Estimation in Biological Fluids. *Biosens. Bioelectron.* **2015***, 68*, 611-616.

(50) Pastor, I.; Esquembre, R.; Micol, V.; Mallavia, R.; Mateo, C. R. A Ready-to-use Fluorimetric Biosensor for Superoxide Radical using Superoxide Dismutase and Peroxidase Immobilized in Sol-Gel Glasses. *Anal. Biochem.* **2004***, 334*, 335-343.

(51) Esquembre, R.; Poveda, J. A.; Mateo, C. R. Biophysical and Functional Characterization of an Ion Channel Peptide Confined in a Sol-Gel Matrix. *J Phys Chem B* **2009***, 113*, 7534-7540.

(52) Esquembre, R.; Pinto, S. N.; Poveda, J. A.; Prieto, M.; Mateo, C. R. Immobilization and Characterization of Giant Unilamellar Vesicles (GUVs) within Porous Silica Glasses. *Soft Matter* **2012***, 8*, 408-417.

(53) Pastor, I.; Salinas-Castillo, A.; Esquembre, R.; Mallavia, R.; Mateo, C. R. Multienzymatic System Immobilization in Sol-Gel Slides: Fluorescent Superoxide Biosensors Development. *Biosens. Bioelectron.* **2010***, 25*, 1526-1529.

(54) Pastor, I.; Ferrer, M. L.; Lillo, M. P.; Gómez, J.; Mateo, C. R. Structure and Dynamics of Lysozyme Encapsulated in a Silica Sol-Gel Matrix. *J Phys Chem B* **2007***, 111*, 11603-11610.

(55) Avnir, D.; Lev, O.; Livage, J. Recent Bio-Applications of Sol-Gel Materials. *J. Mater. Chem.* **2006***, 16*, 1013-1030.

(56) Jin, W.; Brennan, J. D. Properties and Applications of Proteins Encapsulated within Sol-Gel Derived Materials. *Anal. Chim. Acta* **2002***, 461*, 1-36.

(57) Traiphol, R.; Sanguansat, P.; Srikhirin, T.; Kerdcharoen, T.; Osotchan, T. Spectroscopic Study of Photophysical Change in Collapsed Coils of Conjugated Polymers: Effects of Solvent and Temperature. *Macromolecules* **2006***, 39*, 1165-1172.

(58) García Sánchez, F.; Navas Díaz, A.; Ramos Peinado, M. C.; Belledone, C. Free and Sol-Gel Immobilized Alkaline Phosphatase-Based Biosensor for the Determination of Pesticides and Inorganic Compounds. *Anal. Chim. Acta* **2003***, 484*, 45-51.

Graphic for manuscript